Journal of Inclusion Phenomena and Macrocyclic Chemistry **41:** 31–36, 2001.

Molecule-Based Artificial Photosynthesis

YOSHITERU SAKATA*, HIROSHI IMAHORI and KEN-ICHI SUGIURA
Institute of Scientific and Industrial Research, Osaka University, 8-1 Mihogaoka, Ibaraki, Osaka 567-0047, Japan (e-mail: sakata@sanken.osaka-u.ac.jp)

(Received: 15 July 2001; in final form: 31 August 2001)

Key words: C_{60}-(porphyrin)-(ferrocene), porphyrin oligomer with 21 porphyrin units, self-assembled monolayer

Abstract

Guidelines for the design of molecules with a long lifetime of the charge-separated state and for the formation of a self-assembled monolayer were studied by preparing various model compounds linking donor and acceptor with chemical bonds. Based on the obtained results we designed and prepared the SAMs of C_{60}-(porphyrin)-(ferrocene)-$(CH_2)_{11}SH$ on a gold surface and observed a photocurrent with high efficiency (25% quantum yield). In addition, a well-defined, rigid-sheet-structured oligoporphyrin with 21 porphyrin chromophores was prepared as a model for antenna chlorophylls.

Light-energy conversion system

Photosynthesis is the fundamental basis for the life of all organisms on the earth. Therefore, the mimicking of photosynthesis or artificial photosynthesis has been a dream of many scientists, especially of chemists. Although solar-energy conversion systems using silicon have already been developed and are commercially available, molecule-based artificial photosynthesis is still quite attractive and important for the following reasons: (1) there is a good example in nature, where plants are doing molecule-based photosynthesis with high efficiency; (2) molecule-based systems are highly tunable, since organic compounds can be modified easily; (3) the size is nano scale and wide application is expected.

In the natural systems light-energy conversion is carried out by several special chromophores which are fixed and arranged closely to each other in the membrane protein [1]. The selection of the chromophores and their arrangement are optimized to achieve fast forward and slow back electron transfer (ET) in the course of evolution for several billion years. Since the essence of photosynthesis is to produce a long lifetime of the charge-separated state for the conversion of the extra energy into useful energy, the control of ET, i.e., fast forward and slow back ET, is crucial for the development of artificial photosynthetic systems. One of the most useful strategies to get information on how to control ET in synthetic compounds is to prepare suitable model compounds from which the particular controlling factors can be extracted. So far we have prepared a number of porphyrin-linked acceptors from which controlling factors of ET were extracted [2].

Among several factors the following two guidelines are quite important for prolonging the lifetime of the charge-separated state: (1) involvement of a multistep ET process in a molecule. This guideline was recognized by us for the first time by preparing **1** and comparing the lifetime of the charge-separated state with that of **2** [3]. (Lifetimes of **1** and **2** in benzene are 300 and 130 ps, respectively.) Independently and almost at the same time, the same conclusion was obtained by two other groups [4, 5]. Various compounds from diad to pentad for the prolongation of the lifetime of the charged species were examined. The longest lifetime so far achieved is 0.38 sec for **3** in frozen benzonitrile [6]; (2) use of fullerene as an electron acceptor. This requirement was deduced by comparing forward and back ET rates of **4** with respect to **5** [7]. The observed acceleration in forward ET and retardation in back ET as shown in Table 1 was explained by the small reorganization energy of C_{60}. Many experimental and theoretical results supported the explanation [8]. The reasons for the small reorganization energy in fullerenes are the following: (a) An electron in C_{60}^- is delocalized over all carbon atoms sharing a small electron density on each carbon atom. Only a small reorganization for the surrounding solvents is enough in the transformation from C_{60} to C_{60}^-. (b) The C_{60} skelton is rigid enough so that only a small structural charge is accompanied from C_{60} to C_{60}^-. Bearing the above two guidelines in mind, one can design molecules having a long lifetime of the charge-separated state.

* Author for correspondence.

Table 1. Free energy change ($-\Delta G$) and electron transfer rate (k) of charge separation (CS) and charge recombination (CR) in **4** and **5**

	4	**5**
$-\Delta G_{cs}$/eV	0.66	0.96
$k_{cs}/10^{-9}s^{-1}$	9.5	1.5
$-\Delta G_{CR}$/eV	1.40	1.10
$k_{CR}/10^{-9}s^{-1}$	2.0	>50

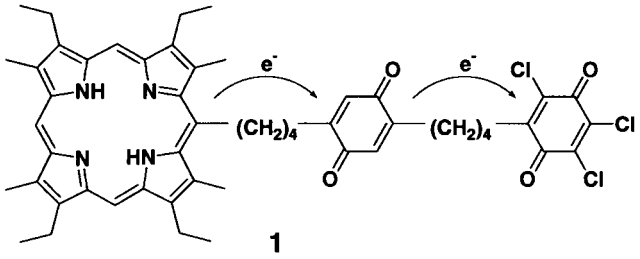

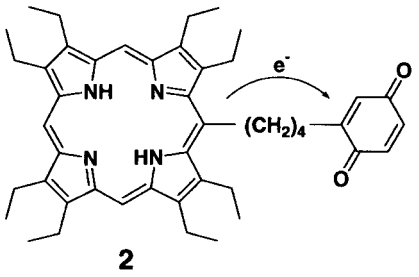

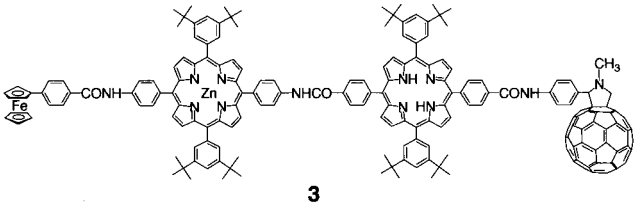

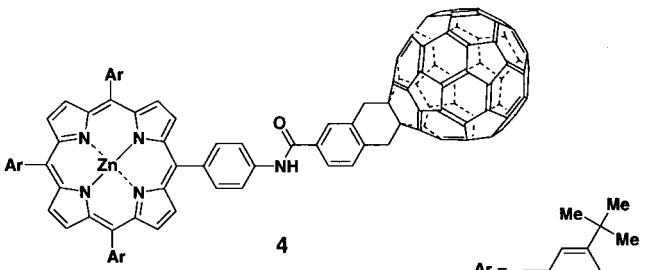

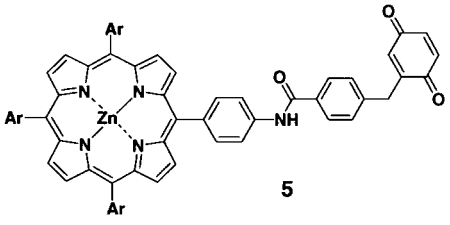

The next step toward artificial photosynthesis is to arrange unidirectionally such a molecular battery and to convert them to useful energy. Among several methods for assembling molecules, self-assembled monolayer (SAM) is the most promising, since it provides a stable membrane with less defects. Therefore, we employed this technique to achieve light-energy conversion.

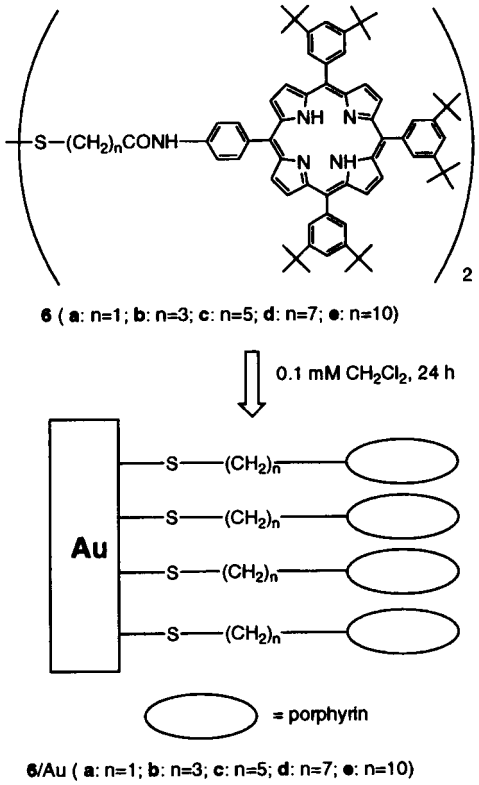

Figure 1. Self-assembled monolayers of porphyrins **6a–e** on gold electrode.

Since the effect of the chain length of the SAMs upon membrane structure was not known in detail, we carried out a systematic investigation on this point [9]. For this purpose disulfides **6** with different spacer lengths were prepared and their structures were characterized using ^{1}H NMR and matrix-assisted laser desorption ionization time of flight mass spectroscopy.

Disulfide **6** having two porphyrin chromophores at both ends of the spacer spontaneously self-assembled to form a monolayer film on a Au(111)/Cr/Si(100) surface as shown in Figure 1. The absorption spectra of **6**/Au are shown in Figure 2. In the figure one can see that the absorbance of the Soret band at around 430 nm increases with an increase of the number of methylenes ($n = 1, 3, 5$), while **6c–e**/Au ($n = 5, 7, 10$) do not exhibit a substantial change in the intensities. Assuming that the molar absorptivities of the band in **6a–e**/Au are similar, the amounts of the adsorbed molecules become saturated at around $n = 5$. The Soret bands are broadened and red-shifted by about 15 nm relative to the corresponding spectra in a dichloromethane solution. The red-shift of the Soret band is probably due to the excitonic coupling among the porphyrin chromophores and aggregation in the monolayer micro environment. A small red-shift (up to 3 nm) was observed for the Soret band as the chain became longer. Probably this shift is due to an increase in the π–π interaction among the porphyrin moieties,

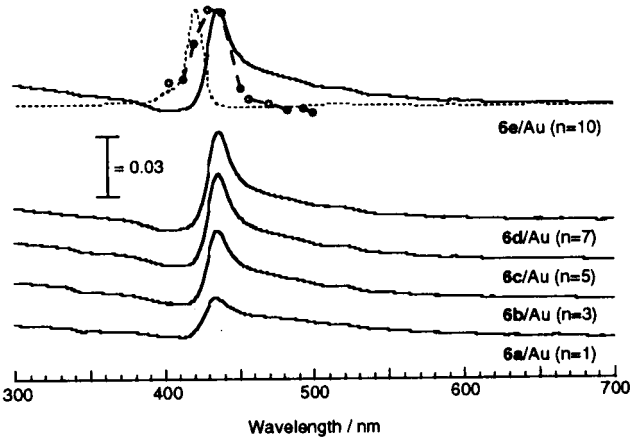

Figure 2. UV-visible absorption spectra of **6a–e**/Au. The absorption spectrum of **6e** in dichloromethane (dotted line) and action spectrum in an Au/**6e**/MV/Pt cell (dashed line with circles) are shown for comparison.

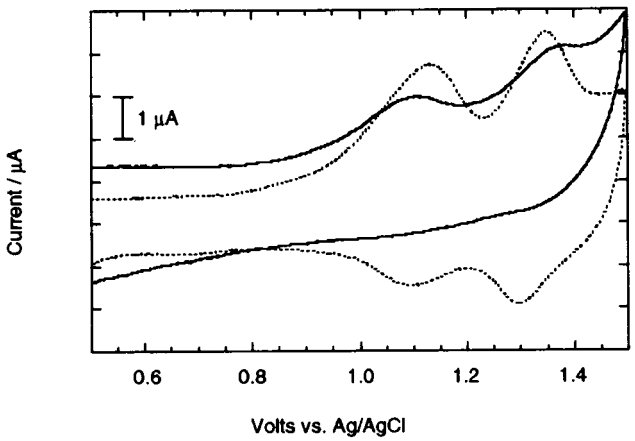

Figure 3. Cyclic voltammograms of **6a**/Au (dotted line) and **6d**/Au (solid line) in dichloromethane.

in spite of the existence of the bulky *tert*-butyl groups at the *meso*-phenyl groups.

Cyclic voltammetry of **6**/Au was carried out in dichloromethane solution containing 0.1 M n-Bu_4NPF_6. Two successive waves, corresponding to the first and the second oxidation of the porphyrin moiety, were clearly observed. The redox waves were irreversible in **6a**/Au, while they were reversible in **6e**/Au. A typical example is shown in Figure 3. The difference between the anodic and cathodic peak potentials (ΔEp = 100–110 mV) are larger than the ideal value (60 mV) indicating slow kinetics of the couple. Integration of the area under the anodic surface waves provides an estimate of the surface coverage, Γ. The results are summarized in Table 2. The values of Γ obtained using the cyclic voltammetry are quite consistent with those using UV-visible absorption spectroscopy. The somewhat smaller Γ values obtained by the absorption method may be attributed to the reduced molar absorptivity of the porphyrin on the gold surface compared with that in the solution. Assuming that the porphyrins are densely packed with a perpendicular orientation to the gold surface, the area of one molecule is calculated to be 200 $Å^2$ (20 Å × 10 Å). The estimated value of the molecular area is in good agreement with those of experimental

Table 2. Surface coverage and molecular occupied area

Entry	n	$\Gamma/10^{11}$ mol cm^{-2a}	Occupied area/$Å^2$ $molecule^{-1b}$	$\Gamma/10^{11}$ mol cm^{-2c}
6a/Au	1	4.4	380	2.1
6b/Au	3	6.4	260	3.9
6c/Au	5	6.6	250	4.9
6d/Au	7	7.9	210	5.4
6e/Au	10	7.7	220	5.0

[a]Estimated on the basis of cyclic voltammetric curve.
[b]Calculated from the value of Γ obtained using cyclic voltammetry.
[c]Estimated using UV-visible absorption spectroscopy.

values for **6d**/Au and **6e**/Au, indicating that densely packed and ordered monolayers are formed in **6d**/Au and **6e**/Au, whereas a less well-ordered structure is formed in **6a–c**. The fact that the values of **6d**/Au and **6e**/Au are somewhat larger than that for the compact packing suggests tilted structures, where the face-to-face stacked porphyrins are inclined to the gold surface with an angle less than 90°.

Photoelectrochemical measurements were performed for **6a–e**/Au in 0.1 M Na_2SO_4 solution containing 5 mM methyl viologen (MV) as an electron carrier using the modified gold electrode as a working electrode, a platinum counter electrode, and a Ag/AgCl reference electrode. In the three-electrode systems, an increase in the cathodic photocurrent with an increase of the negative bias to the gold electrode demonstrates that the photocurrent flows from the cathode to the anode through the electrode. The photocurrent produced by on-off illumination of the Au/**6a–e**/MV/Pt cell is shown in Figure 4. The intensities of the short-circuit photocurrents for the Au/**6**/MV/Pt cell are an order of magnitude larger than those of the Au/**6**/Pt cell indicating the involvement of MV in the former case. The good agreement between the action spectrum and the absorption in the range of 400–500 nm as shown in Figure 2 shows that the porphyrin is the photoactive species. The SAM showed a photoelectric response when switching the light on and off. The intensity of the photocurrent from the Au/**6**/MV/Pt cell decreased as the alkane chain length decreased, and eventually a negative photocurrent was observed in the Au/**6a**/MV/Pt cell. A similar negative photocurrent was also observed in bare Au/MV/Pt and bare Au/Pt cells, indicating that direct excitation of the bare gold electrode is mainly responsible for the small negative photocurrent.

The photocurrent generation trend can be explained using the following mechanism. An electron transfer takes place from the excited singlet or triplet state of the porphyrin to the MV. The reduced MV diffuses to the Pt electrode and transfers the electron, generating the photocurrent. However, there may be a competitive deactivation pathway in the excited porphyrin by the gold electrode. As the number of methylenes decreases, electronic coupling between the porphyrin and the electrode increases, leading to the efficient quenching of the excited porphyrin by the gold surface, probably via energy transfer or electron transfer through the spacer. Therefore, it is concluded that the dramatic decrease of the photocurrent with a decrease of the alkyl chain length

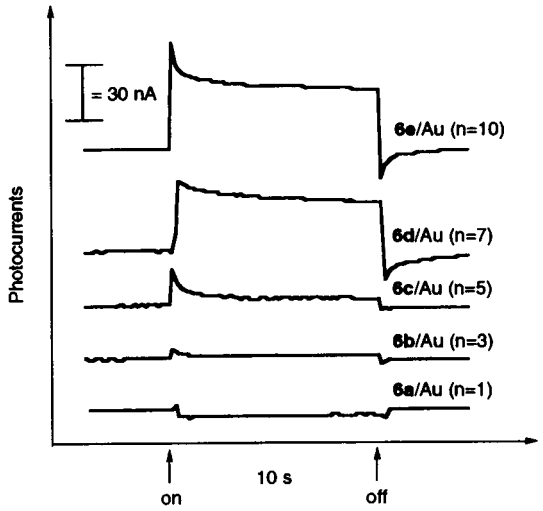

Figure 4. Photocurrents irradiated with a monochromic light of 438.5 nm upon **6a–e**/Au.

is responsible for the more efficient quenching of the excited porphyrin by the electrode rather than the slight decrease in the amount of the adsorbed molecules on the gold surface.

From the above experiments we obtained the third guideline to design a molecule that has a long-lived charge-separated state and can assemble to form monolayer. The guideline implies that alkanethiols with a long alkyl chain ($n = 10$) are required as a terminal substituent in a photoactive molecule. Bearing these in mind, we designed a triad **7**, where the above three requirements, i.e., multi-step ET process, C_{60} as an electron acceptor, and an alkane thiol with a long alkyl chain, are included [10].

Similar to the procedure described for **6**/Au, SAM **7**/Au was prepared and characterized. The occupied area of one molecule in **7**/Au was obtained from the area of the anodic peak of the ferrocene to be 86 $Å^2$ molecule^{-1}. Assuming that the triad is densely packed perpendicularly to the gold surface, the occupied area is calculated to be ca 87 $Å^2$ for hexagonal packing of the C_{60} moities, which is in good agreement with the experimental value. Therefore, it was concluded that the triad molecules in **7**/Au are well-packed with an almost perpendicular orientation on the gold surface. The cyclic voltammetric current-potential (I–V) responses for a bare gold electrode, **7**/Au with 1 mM $Fe(CN)_6^{3-}$ as an electroactive species and 1.0 M $NaClO_4$ as an electrolyte. There is a dramatic difference between the I–V responses for the bare gold and the monolayer-covered electrode. A reversible cyclic voltammogram of the redox probe was clearly observed for the bare electrode, implying that the redox probe exhibits electrical communication with the bare gold electrode. In contrast, such communication decreases dramatically for **7**/Au and becomes irreversible. These data clearly show that the redox communication of $Fe(CN)_6^{3-}$ is interfered by the triad SAM of **7** due to the densely packed structure.

Photoelectrochemical measurements using **7**/Au in an O_2-staturated 0.1 M Na_2SO_4 solution were carried out in a three-electrode system, which is identical to the previously described one for **6**/Au. A cathodic photoelectrochemical response was observed when the light was switched on and off. The intensity of the photocurrent in **7**/Au is stronger by 2 orders of magnitude than that of **6**/Au under the same conditions. This implies that the C_{60} and the ferrocene moieties are responsible for the higher efficiency. The quantum yield is evaluated to be 25%, which is about two times larger than the highest quantum efficiency (12%) ever reported for the photoinduced multistep ET at the monolayer-modified metal electrodes and across the artificial membranes using donor-acceptor linked molecules under similar conditions.

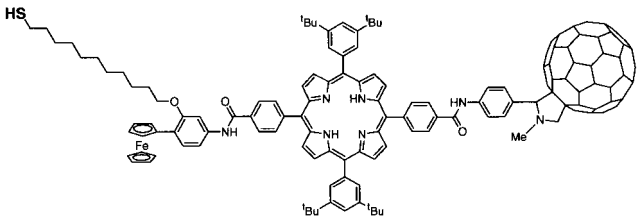

7

In natural systems the solar-energy-conversion apparatus is coupled with the light-harvesting system. Mimicking this situation we installed an energy transfer (EN) system in the previous **7**/Au system [11]. We selected a boron-dipyrrin dye **8** as an energy donor, since it can transfer efficiently its energy to the porphyrin in **7**. Mixed SAMs composed of **7** and **8** with different ratios were prepared similar to the method for **6**/Au and **7**/Au. On the basis of cyclic voltammetry and absorption spectra, the surface coverage of **7** and **8** was determined. It turned out that **7** and **8** are densely packed on the gold surface in the mixed SAMs (**7**, **8**/Au). The photoelectrochemical measurements were performed for Au/**7**, **8**/MV^{2+}/Pt cell under the optimized conditions. The action spectra of Au/**7**, **8** (50:50)/MV^{2+}/Pt cell and Au/**7**/MV^{2+}/Pt cell together with the absorption spectrum of **7**, **8** (50:50)/Au are shown in Figure 5. The Au/**7**, **8** (50:50)/MV^{2+}/Pt cell shows a cathodic photoelectrochemical response from both the triad **7** (430 nm) and boron-dipyrrin **8** units (510 nm), which agree with the absorption of **7**, **8** (50:50)/Au. Figure 5 shows clearly that the photocurrent generation efficiency of the Au/**7**, **8** (50:50)/MV^{2+}/Pt cell at 510 nm is much larger than that of the Au/**7**/MV^{2+}/Pt cell at the same wavelength. The quantum yields were determined to be 45 ± 8% at 510 nm for the Au/**7**, **8** (25:75)/MV^{2+}/Pt cell. The maximum value of the quantum yield was obtained to be 50 ± 8% at 510 nm for the Au/**7**, **8**(25:75)/MV^{2+}/Pt cell. The quite high efficiency in the light-energy conversion, observed in the above experiments, shows that molecule-based artificial photosynthesis is quite promising in the future.

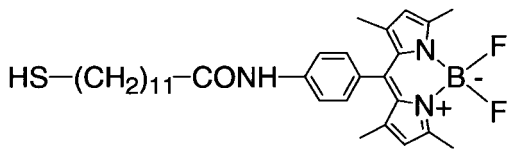

8

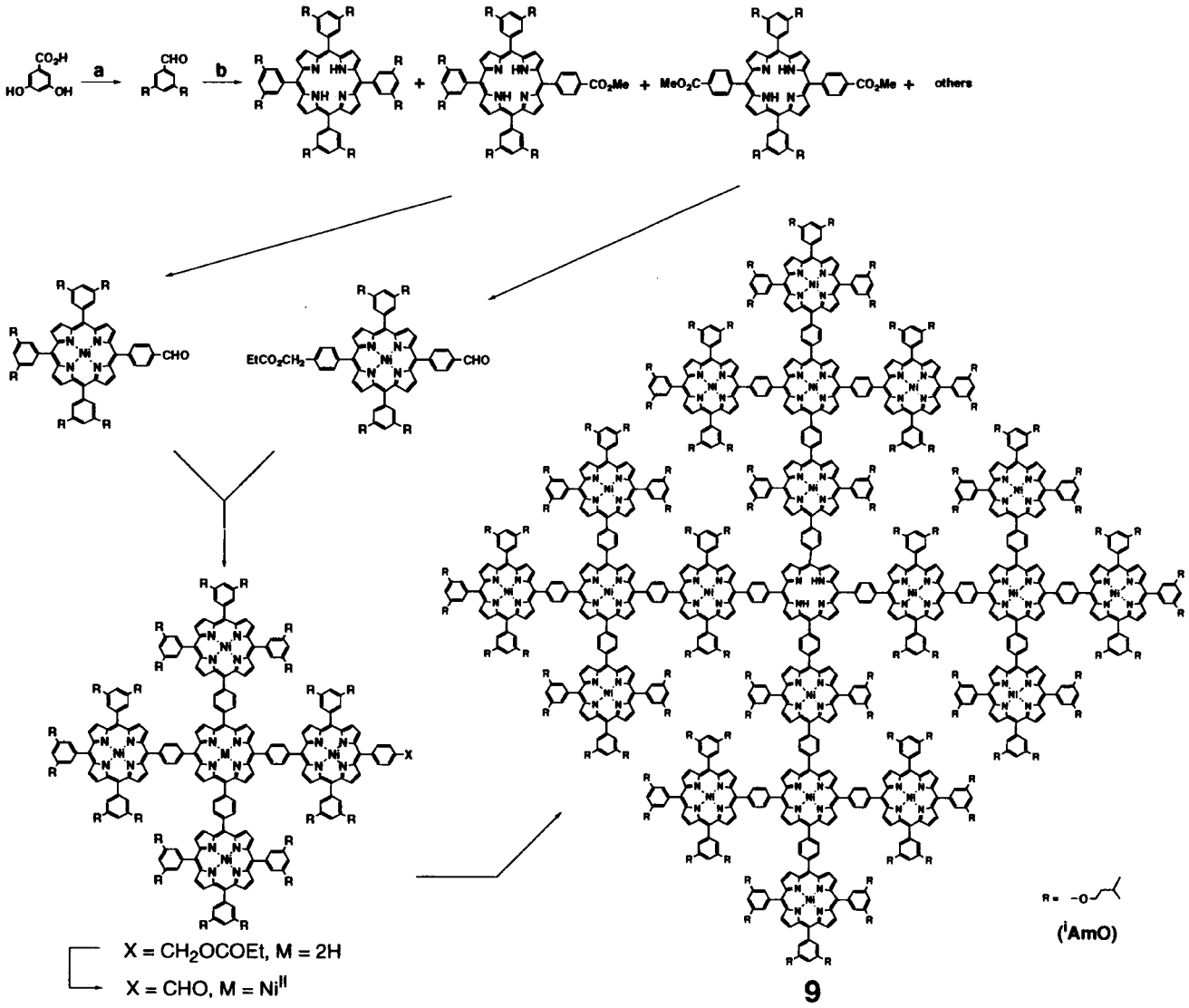

Scheme 1.

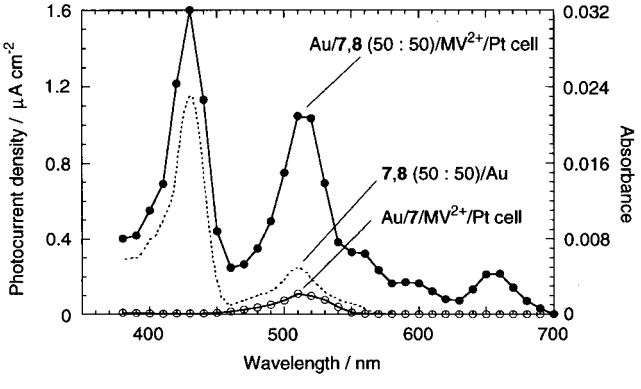

Figure 5. Action spectra of Au/**7, 8** (50 : 50)/MV^{2+}/Pt cell (solid line with black circles) and Au/**7**/MV^{2+}/Pt cell (solid line with white circles) and the absorption spectrum (dotted line) of a mixed SAM of **7** and **8** on a gold surface (**7,8** (50 : 50)/Au).

Artificial light-harvesting system

As described above, energy transfer is quite important to achieve efficient light-energy conversion. Although there exist a number of excellent artificial compounds for light-energy conversion, the number of synthetic models for light harvesting is limited. A sophisticated arrangement of oligoporphyrins in the natural system is responsible for the efficient EN. In an attempt to mimic the function we have designed and synthesized a well-defined, rigid-sheet-structured oligoporphyrin **9** with 21 porphyrin chromophores [12]. The synthetic route of **9** is summarized in Scheme 1. The structure of **9** was characterized by MULDI-TOF mass an UV-vis spectra. Additional evidence for the structure was obtained by the direct observation of the molecular shape using STM. The STM image consists of 21 major lobes aligned in a perfectly square shape, whose size is 95 Å along the diagonal and 65 Å along the side, which are in good agreement with the calculated values, 93.3 and 65.7 Å, respectively.

Acknowledgement

This work was supported by COE and Grant-in-Aid No.12440199 and by Scientific Research on Priority Area of

Creation of Delocalized Electronic Systems from the Ministry of Education, Culture, Sports, Science and Technology, Japan. Y.S. thanks the Mitsubishi Foundation for financial support.

References

1. J. Deisenhofer, O. Epp, K. Miki, R. Huber, and H. Michel: *J. Mol. Biol.* **180**, 385 (1994).
2. Y. Sakata, H. Imahori, H. Tsue, S. Higashida, T. Akiyama, E. Yoshizawa, M. Aoki, K. Yamada, K. Hagiwara, S. Taniguchi, and T. Okada: *Pure & Appl. Chem.* **69**, 1951 (1997).
3. S. Nishitani, N. Kurata, Y. Sakata, S. Misumi, A. Karen. T. Okada, and N. Mataga: *J. Am. Chem. Soc.* **105**, 7771 (1983).
4. T.A. Moore, D. Gust, P. Mathis, J.-C. Mialocq, C. Chachaty, R. V. Bensasson, E.J. Land, D. Doizi, P.A. Liddell, W.R. Lehman, G.A. Nemlth, and A.L. Moore: *Nature* **307**, 630 (1984).
5. M.R. Wasielewski, M.P. Niemczyk, W.A. Svec, and E.B. Pewitt: *J. Am. Chem. Soc.* **107**, 5562 (1985).
6. H. Imahori, D.M. Guldi, K. Tamaki, Y. Yoshida, C. Luo, Y. Sakata, and S. Fukuzumi: *J. Am. Chem. Soc.* **123**, 6617 (2001).
7. H. Imahori, K. Hagiwara, T. Akiyama, M. Aoki, S. Taniguchi, T. Okada, M. Shirakawa, and Y. Sakata: *Chem. Phys. Lett.* **263**, 545 (1996).
8. H. Imahori and Y. Sakata: *Eur. J. Org. Chem.* **2445** (1999).
9. H. Imahori, H. Norieda, S. Ozawa, K. Ushida, H. Yamada, T. Azuma, K. Tamaki, and Y. Sakata: *Langmuir* **14**, 5335 (1998).
10. H. Imahori, H. Yamada, Y. Nishimura, I. Yamazaki, and Y. Sakata: *J. Phys. Chem. B* **104**, 2099 (2000).
11. H. Imahori, H. Norieda, H. Yamada, Y. Nishimura, I. Yamazaki, Y. Sakata, and S. Fukuzumi: *J. Am. Chem. Soc.* **123**, 100 (2001).
12. K. Sugiura, H. Tanaka, T. Matsumoto, T. Kawai, and Y. Sakata: *Chem. Lett.* 1193 (1999).